

Identification of mechanism of the oncogenic role of FGFR1 in papillary thyroid carcinoma

Xiong Bing Li,^{1*} Jia Li Li,^{2*} Chao Wang,¹ Yong Zhang,¹ Jing Li³

¹Department of Oncology

²Department of Endocrinology

³Department of Nephrology, Xianning Central Hospital, The First Affiliated Hospital of Hubei University of Science and Technology, Xianning, China

*These authors equally contributed

ABSTRACT

Papillary thyroid carcinoma (PTC) is the most prevalent malignancy of the thyroid. Fibroblast growth factor receptor 1 (FGFR1) is highly expressed in PTC and works as an oncogenic protein in this disease. In this report, we wanted to uncover a new mechanism that drives overexpression of FGFR1 in PTC. Analysis of FGFR1 expression in clinical specimens and PTC cells revealed that FGFR1 expression was enhanced in PTC. Using siRNA/shRNA silencing experiments, we found that FGFR1 downregulation impeded PTC cell growth, invasion, and migration and promoted apoptosis *in vitro*, as well as suppressed tumor growth *in vivo*. Bioinformatic analyses predicted the potential USP7-FGFR1 interplay and the potential binding between YY1 and the FGFR1 promoter. The mechanism study found that USP7 stabilized FGFR1 protein *via* deubiquitination, and YY1 could promote the transcription of FGFR1. Our rescue experiments showed that FGFR1 re-expression had a counteracting effect on USP7 downregulation-imposed *in vitro* alterations of cell functions and *in vivo* suppression of xenograft growth. In conclusion, our study identifies the deubiquitinating enzyme USP7 and the oncogenic transcription factor YY1 as potent inducers of FGFR1 overexpression. Designing inhibitors targeting FGFR1 or its upstream inducers USP7 and YY1 may be foreseen as a promising strategy to control PTC development.

Key words: papillary thyroid carcinoma; FGFR1; deubiquitination; transcription factor; inhibitors.

Correspondence: : Jing Li, Department of Nephrology, Xianning Central Hospital, The First Affiliated Hospital of Hubei University of Science and Technology, No. 288, Jingui Road, Xianning 437100, China.
E-mail: lijing316013329@163.com

Contributions: XBL, experiments performing, manuscript original drafting; JLL data collection and analysis; YZ, JL, CW, study design and supervision, contribution to methodology, instruments' software operation, manuscript editing. All the authors read and approved the final version of the manuscript and agreed to be accountable for all aspects of the work.

Conflict of interest: the authors declare that they have no competing interests, and all authors confirm accuracy.

Ethics approval and consent to participate: the Xianning Central Hospital Institutional Ethics Committee approved the use of the human specimens (No. TDLL202209-06). All participants signed informed consent for study participation. This study was approved by the Xianning Central Hospital Animal Care and Use Committee (IACUC, No. ANHB202303-08).

Availability of data and materials: data is available from the corresponding author upon reasonable request.

Funding: None.

Introduction

As the most prevalent cancer of the thyroid, papillary thyroid carcinoma (PTC) has an increased trend of incidence in recent years.¹ In China, the cases of this tumorigenic disease have been on the rise.² Although the diagnostic techniques and treatment options for patients with PTC have generally improved, there is still an urgent need for more innovative and efficient targets for PTC diagnosis and treatment due to the rapidly increased number of cases. Thus, essential players in PTC development, including oncogenic proteins, deserve to be explored.

Fibroblast growth factor receptor 1 (FGFR1), a member of the FGFR family, is capable of inducing the activation of downstream signaling pathways, including the PI3K and MAPK pathways, thereby actively participating in cell differentiation, growth, motility, and survival.³⁻⁵ Overexpression of FGFR1 and abnormal activation of the FGFR1 signaling have been frequently found in various cancer types, such as breast cancer, squamous cell lung cancer, and bladder tumor.⁶⁻⁸ In cancer, FGFR1 exerts pro-tumorigenic activity, and FGFR1 inhibitors have been well-known for anti-cancer therapy.⁹ Furthermore, the genomic alteration of FGFR1 occurs in PTC,¹⁰ and FGFR1 can contribute to PTC malignant phenotypes.¹¹

Ubiquitination and deubiquitination, vital determinators of protein fate, take part in tumor biology by mediating post-translational modification.¹² The FGFR1 signaling can be downregulated by the ubiquitination of FGFR1.¹³ Through the recognition of specific DNA sequences, transcription factors (TFs) can control the transcription of the genome.¹⁴ TFs Runx2 and NF- κ B have been shown to target FGFR1 and guide FGFR1 transcription.^{3,15}

Given the overexpression and oncogenic action of FGFR1 in PTC,^{11,13} we wanted to uncover a new post-translational modifier based on deubiquitination, a process that promotes protein stability,¹⁶ and a novel oncogenic TF, both of which drive FGFR1 overexpression in PTC. Based on the observations of bioinformatics analysis, we hypothesized that the deubiquitinating enzyme USP7, which works as a tumor driver in PTC by stabilizing oncogenic proteins,¹⁷ and the TF YY1, which is a contributor to PTC by enhancing oncogene transcription,¹⁸ might contribute to FGFR1 overexpression, thereby accelerating PTC development.

Materials and Methods

Clinical specimens

We obtained surgically resected samples, including tumor specimens and neighboring healthy thyroid samples, from 32 patients with confirmed PTC in Xianning Central Hospital from August 2021 to May 2023. All clinical specimens were divided into two parts: one was fixed with 4% paraformaldehyde for FGFR1 immunohistochemical staining, and the other part for expression analysis was stored in RNAlater reagent (Beyotime, Shanghai, China) at -80°C . The Xianning Central Hospital Institutional Ethics Committee approved the use of the human specimens (no. TDLL202209-06), and all participants signed informed consent for study participation.

Cell lines and transfection and transduction of cell lines

Cell lines used in this study included normal Nthy-ori3-1 (#IM-H512; Immocell, Xiamen, China), TPC-1 PTC (#CL-0643; Procell, Wuhan, China), IHH-4 PTC (#CL-0803; Procell) and SW579 PTC (#CL-0224B; Procell) cell lines. Cell culture was car-

ried out in an 85% humidity incubator with a fixed concentration of CO_2 (5%) at 37°C using RPMI-1640 (Solarbio, Shanghai, China) for Nthy-ori3-1, IHH-4, and TPC-1 cells and DMEM (Procell) for SW579 cells, which were enriched with 1% antibiotics (Beyotime) and 10% FBS (EuroClone, Milan, Italy). MG132 (Selleck, Shanghai, China), a repressor of ubiquitin-proteasome,¹⁹ was used to incubate TPC-1 and SW579 cells at a 100 nM concentration for 24 h.

For knockdown experiments, we obtained FGFR1-siRNA (si-FGFR1), USP7-siRNA (si-USP7), YY1-siRNA (si-YY1), and scrambled siRNA sequence (si-NC) from Genscript (Nanjing, China), as well as lentivirus coding USP7-shRNA (sh-USP7) or scrambled shRNA (sh-NC) from BioHealth (Wuhan, China). The pCMV-FGFR1(human)-3 \times Flag-Neo obtained from Miaoling (Wuhan, China) was used to encode the FGFR1 protein in rescue experiments. For *in vitro* analyses, TPC-1 and SW579 cells (5×10^4 cells for 1st transfection) were subjected to transfection of si-FGFR1 (30 nM), si-USP7 (30 nM), si-YY1 (30 nM), si-USP7 (15 nM) along with the FGFR1 plasmid (500 ng), or si-NC control (30 nM) under the use of Lipofectamine 2000 following the reagent instructions (Life Technologies, Abingdon, UK). For *in vivo* studies, SW579 cells were infected with sh-USP7 or sh-NC lentivirus. After transduction, cells were processed by puromycin selection (2 $\mu\text{g}/\text{mL}$) for two weeks.

Xenograft studies

With the approval of the Xianning Central Hospital Animal Care and Use Committee (IACUC, No. ANHB202303-08), we used 18 female BALB/c nude mice (1.5- to 2-month-old; Aniphe BioLab, Nanjing, China) in xenograft experiments, which were grouped into three groups: sh-USP7 (n=6), sh-USP7+FGFR1 (n=6), and sh-NC (n=6). To examine the influence on xenograft growth, we injected sh-USP7 or sh-NC lentivirus-transduced SW579 cells (7×10^6 cells per mouse) into the left flank of mice by subcutaneous implantation. One week later, the formed sh-USP7 xenografts in the sh-USP7+FGFR1 group were subjected to intratumor injection of 1 μg FGFR1 plasmid. We measured tumor width and length using a pair of callipers every three days and determined xenograft volume through the width² \times length \times 1/2 formula. When the mice were sacrificed on day 23 after subcutaneous implantation, all xenografts were harvested and subjected to the indicated analyses.

Immunohistochemical staining

Paraformaldehyde-fixed, paraffin-embedded human clinical specimens and mouse xenografts were processed by immunohistochemical staining as described by Hu *et al.*²⁰ Briefly, tissues were fixed in 4% paraformaldehyde, embedded in paraffin, and sectioned (4-5 μm). After that, tissues were rehydrated and subjected to antigen retrieval in sodium citrate solution (pH=6.0; Servicebio), followed by non-specific blocking in 3% hydrogen peroxide. The mouse anti-FGFR1 monoclonal (#60325-1-Ig, 1:300) and rabbit anti-Ki67 polyclonal (#27309-1-AP, 1:5000) primary antibodies (Proteintech, Wuhan, China) were applied overnight at 4°C to probe FGFR1 and Ki67, respectively. A rabbit antibody against IgG (#30000-0-AP, 1:5000; Proteintech) was used as the negative control. Sections were then incubated with anti-mouse (#ab6728, 1:800) and anti-rabbit (#ab7090, 1:2000) secondary antibodies (Abcam, Cambridge, UK) labeled by HRP for 50 min at room temperature. For the development of signals, we applied the DAB kit (Solarbio) before counterstaining with hematoxylin. At least five random fields were obtained under the Axiovert 200M microscope (Zeiss, Oberkochen, Germany). Each sample consisted of 10 consecutive slices. The percentage of positive expression cells was determined relative to the total cell count.

mRNA analysis by quantitative PCR

We prepared total RNA from 50 mg of human specimens (including tumors and neighboring normal tissues) and 5×10^6 si-USP7- or si-NC-transfected TPC-1 and SW579 PTC cells using the NucleoSpin[®] RNA II Kit and accompanying directions (Macherey-Nagel, Düren, Germany). After quantification by spectrophotometric measurement, 500 ng of each RNA extract was randomly primed for cDNA generation using the ReverTra Ace RT Kit as suggested by the producer (Toyobo, Tokyo, Japan). Using generated cDNA with a 20-fold dilution as template, we performed quantitative PCR to evaluate FGFR1 mRNA expression using SYBR Green (Vazyme, Nanjing, China) with a primer set (5'-GACGCAGGGGAGTATACGTG-3'-forward and 5'-ACTG-GAGTCAGCAGACTG-3'-reverse). The GAPDH served as a loading control with a universal primer (5'-AGAAG-GCTGGGGCTCATTTG-3'-forward and 5'-AGGGGCCATC-CACAGTCTTC-3'-reverse). Ct values were averaged from triplicate reactions, and the $2^{-\Delta\Delta C_t}$ formula was used to calculate relative expression.

Protein analysis by immunoblotting

Using the AllPrep DNA/RNA/Protein kit, human clinical specimens and cell lines were extracted for total protein as recommended by the vendor (Qiagen, Crawley, UK). Utilizing standard methods described by Yao and colleagues,²¹ we conducted immunoblots using mouse anti-FGFR1 monoclonal (#60325-1-Ig, 1:1500; Proteintech), mouse anti-USP7 monoclonal (#66514-1-Ig, 1:10000; Proteintech), rabbit anti-YY1 monoclonal (#ab232573, 1:1000; Abcam), and rabbit anti-GAPDH polyclonal (#10494-1-AP, 1:20000; Proteintech) antibodies, as well as secondary antibodies conjugated by HRP. After signal development using Supersignal West Dura (Thermo Fisher Scientific, Geel, Belgium), we analyzed gray level using the iBright 1500 System (Thermo Fisher Scientific).

Evaluation of cell growth

Growth of TPC-1 and SW579 PTC cells that were introduced with si-FGFR1, si-USP7, si-USP7+FGFR1, or si-NC was determined by assessing viability *via* the CCK-8 experiment (MCE, Shanghai, China) and proliferation *via* the EdU staining assay (BeyoClick[™] EdU-488, Beyotime). In brief, we seeded TPC-1 and SW579 PTC cells in a 96-well plastic plate and maintained them for 8-12 h, followed by the described transfection. In the CCK-8 experiment, the CCK-8 working solution was used for cell incubation as per the vendor's description. We gauged the absorbance per sample through a 96-well spectrometer (BMG Labtech, Ortenberg, Germany). In the EdU staining experiment, cells after 48 h of transfection were first treated with the EdU working reagent and then stained with Click Additive 488 Solution. After nucleus counterstaining with DAPI (Beyotime), we obtained fluorescent images under a Fluoview FV1000 microscope (Olympus, Mishima, Japan). The ratio of EdU positive cells (showing a green fluorescence) was determined relative to the total cell count (showing a blue fluorescence).

Detection of cell apoptosis, invasiveness, and migratory ability

TPC-1 and SW579 PTC cells introduced with si-FGFR1, si-USP7, si-USP7+FGFR1, or si-NC were subjected to these analyses. For apoptosis analysis by flow cytometry, cells after 48 h of transfection were doubly stained with PI and FITC-Annexin V (Vazyme) in accordance with the vendor's protocols. We defined apoptotic cells as positive for Annexin V. For invasiveness analysis by transwell assay, we seeded PTC cells after 48 h of transfection into the upper chamber of a 24-Transwell plate (Corning,

Lindfield, NSW, Australia) and added 650 μ L of 10% FBS medium into the bottom. Eighteen hours later, we counted the invaded cells under an inverted microscope. For motility analysis by wound healing assay, we plated transfected PTC cells in 6-well plastic plates. When cells reached almost 100 confluence, we made a vertical wound *via* pipette tips (200 μ L) and continued to culture cells in media containing mitomycin C (10 μ g/mL) for 24 h, to inhibit cell proliferation. We captured images at 0 h and 24 h for evaluation of cell migratory ability. At least three random fields for each sample were obtained under the Axiovert 200M microscope. The wound width was measured by ImageJ software (National Institutes of Health, Bethesda, MD, USA), and the relative migration distance was determined based on that of un-transfected cells.

Bioinformatics

We utilized Ubibrowser 2.0 database²² to predict deubiquitinase-FGFR1 interactions (http://ubibrowser.bio-it.cn/ubibrowser_v3/). Jasp²⁰²⁴ predicted the putative binding between YY1 and the FGFR1 promoter (<https://jasp.elixir.no/>).

Immunoprecipitation assay

We determined the influence of USP7 in FGFR1 deubiquitination by an immunoprecipitation experiment with recombinant anti-Flag antibody (#80010-1-RR, 1 μ g for 1 mg of protein extract; Proteintech) and subsequent immunoblot analysis using rabbit ubiquitin polyclonal antibody (anti-Ub, #10201-2-AP, 1:5000; Proteintech). Briefly, TPC-1 cells were co-transfected with the FGFR1 plasmid fused with 3 \times Flag tags and si-USP7 or sh-NC control, followed by lysing in RIPA buffer (Beyotime) containing PMSF (Servicebio, Wuhan, China). Total cell extract was subjected to incubation with the anti-Flag antibody and Protein A/G agarose (Thermo Fisher Scientific). The immunoprecipitates were collected for the evaluation of Ub linked to the Flag-FGFR1 protein by immunoblotting to determine ubiquitinated FGFR1.

Immunofluorescence and colocalization assay

Si-USP7- or si-NC-introduced TPC-1 cells were subjected to fixation with 4% paraformaldehyde, permeation with 0.5% Triton X-100 in PBS, and blocking with 3% BSA (Servicebio). The primary antibodies, including rabbit anti-FGFR1 polyclonal (#GB115541, 1:100; Servicebio) and mouse anti-USP7 monoclonal (#66514-1-Ig, 1:300; Proteintech), were used prior to the application of Alexa 488-labeled anti-mouse (#GB25301, 1:500; Servicebio) and Cy3-labeled anti-rabbit (#GB21303, 1:500; Servicebio) IgG secondary antibodies following the vendors' guidelines. For nucleus counterstaining, DAPI reagent was applied. Under the Fluoview FV1000 microscope, we captured fluorescent images at 400 \times magnification.

Chromatin immunoprecipitation experiment

We evaluated the binding of YY1 and the FGFR1 promoter under the use of chromatin immunoprecipitation (ChIP) experiments with the BeyoChIP[™] Enzymatic ChIP Kit and instructions (Beyotime). Briefly, TPC-1 and SW579 cells subjected to formaldehyde and glycine solution processing were re-suspended in PBS plus PMSF. Following the instructions, we prepared the cell nucleus and applied 1 μ L of MNase for chromatin fragmentation. Using mouse anti-YY1 monoclonal (#66281-1-Ig, 0.5 μ g for 1 mg of cell extract; Proteintech) or normal rabbit IgG polyclonal (#30000-0-AP, 0.5 μ g for 1 mg of cell extract; Proteintech) antibody, the precipitates were pulled down by Protein A/G agarose for measurement of enrichment content of the FGFR1 promoter by quantitative PCR.

Luciferase assay

We analyzed the regulatory function of YY1 in FGFR1 transcription using luciferase assay by generating reporter constructs including wild-type (WT) and mutant (MUT) FGFR1 reporter (WT-FGFR1 and MUT-FGFR1), which were made by inserting the 500-bp length fragment of the FGFR1 promoter encompassing the predicted WT sequence or MUT sequence into the pGL3 vector (HonorGene, Changsha, China). WT-FGFR1 or MUT-FGFR1 was co-introduced into TPC-1 and SW579 cells along with the pRL-TK *Renilla* control plasmid (Promega, Milan, Italy) and si-YY1 or si-NC mock. Cells after 48 h of transfection were used for luciferase activity analysis with the Dual-Lucy Assay Kit (Solarbio). We expressed relative activity as the ratio of firefly to *Renilla* luciferase.

Statistical analysis

We presented all data as means of at least three biological replicates with standard deviation (means \pm SD). Significance for all the tests, evaluated by calculating the *p*-value using an unpaired Student's *t*-test (for two group comparison) or ANOVA (for multiple analysis), was <0.05 .

Results

FGFR1 expression is enhanced in human PTC

FGFR1 has garnered great attention in PTC due to its important significance in disease development.^{11,13} To evaluate the exact role of FGFR1 in human PTC, we began by determining its expression in PTC samples. Immunohistochemical staining confirmed elevated FGFR1 expression in PTC tumors (Figure 1A). Our quantitative PCR and immunoblot analyses showed increased FGFR1 expression at both mRNA and protein levels in these primary tumors versus their neighboring normal tissues (Figure 1 B,C). Importantly, FGFR1 protein levels were highly upregulated in PTC cell lines (IHH-4, TPC-1, and SW579) relative to the normal Nthy-ori3-1 cell line (Figure 1D). The above results confirm the overexpression of FGFR1 in human PTC.

Downregulation of FGFR1 impedes PTC cell growth, invasion, and migration and promotes apoptosis

We then studied the biological functions of FGFR1 in PTC using TPC-1 and SW579 cells, which presented more significant elevation in FGFR1 protein (Figure 1D). A FGFR1-siRNA (si-FGFR1) that was validated to successfully knock down FGFR1 in

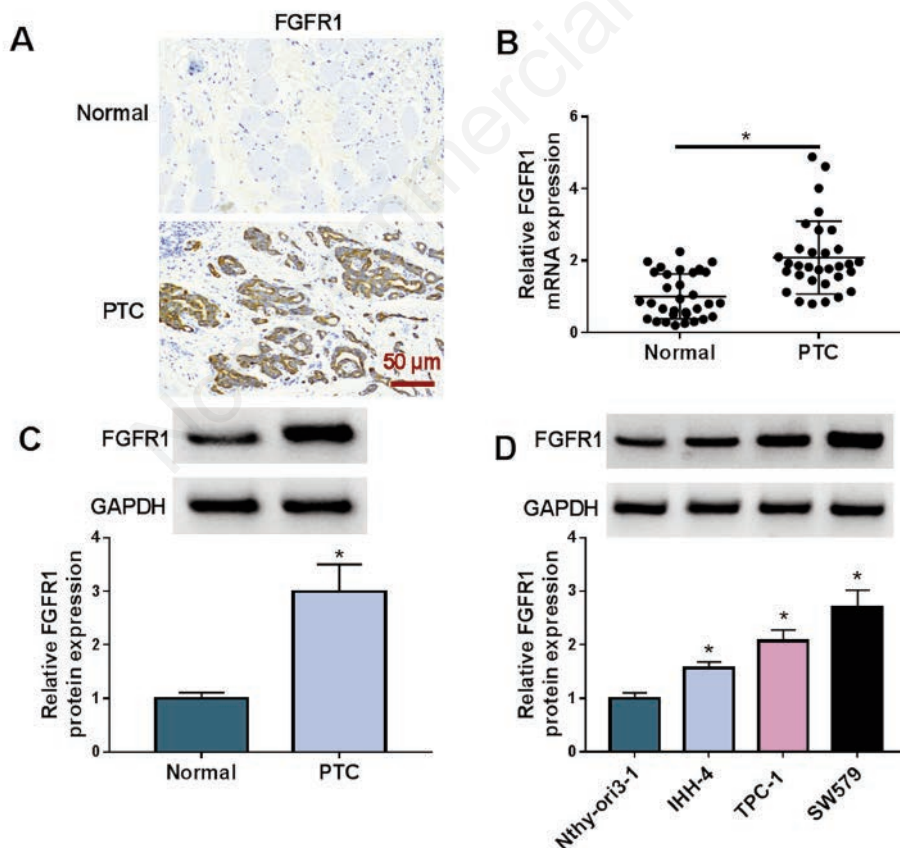


Figure 1. Enhanced expression of FGFR1 in human PTC. **A**) Representative immunohistochemical staining of PTC tumors (n=3) and neighboring healthy thyroid samples (n=3). **B,C**) Quantitative PCR by RT-qPCR of FGFR1 mRNA (**B**) and immunoblots of FGFR1 protein expression (**C**) in PTC tumors (n=32) and neighboring healthy thyroid samples (n=32). **D**) Representative immunoblot analysis of three PTC cell lines (IHH-4, TPC-1, and SW579) and control cell line Nthy-ori3-1 to detect FGFR1 protein levels. * $p<0.05$.

the two PTC cell lines was used in this study (Figure 2A). si-FGFR1-introduced PTC cells (both TPC-1 and SW579) displayed suppressed cell viability and reduced the ratio of EdU positive cells (Figure 2 B,C), indicating that downregulation of FGFR1 results in an inhibition in PTC cell growth. Flow cytometry revealed that FGFR1 downregulation could drive apoptosis of TPC-1 and SW579 PTC cells compared with the nontarget control si-NC (Figure 2D). We then utilized transwell and wound healing assays to evaluate the effect on cell invasiveness and migratory ability, respectively. TPC-1 and SW579 cells with FGFR1 downregulation presented suppressed invasiveness (Figure 2 E,F) and weakened migratory ability (Figure 2G). Together, and in agreement with previous documents,^{11,13} these findings demonstrate that dysregulated FGFR1 can cause PTC development.

USP7 stabilizes FGFR1 *via* deubiquitination

In order to determine what drives FGFR1 overexpression in PTC, we first considered the post-translational modifiers. The deubiquitinating enzyme USP7 is frequently overexpressed in many cancer types and has been identified as a tumor promoter due to its regulation in various oncogenic proteins through deubiquitination.^{23,24} Unsurprisingly, when we used the Ubibrowser 2.0 database²² to predict deubiquitinase-FGFR1 interplays, we found that USP7 had a potential to stabilize FGFR1 (Figure 3A). To address this possibility, the regulation of USP7 in FGFR1 expression was examined. Reduced USP7 protein expression upon transfection of a USP7-siRNA (si-USP7), confirmed by immunoblot

analysis (Figure 3B), did not alter the mRNA expression of FGFR1 in TPC-1 and SW579 PTC cells compared to the si-NC control (Figure 3C). Interestingly, PTC cells with USP7 silencing exhibited reduced FGFR1 protein level (Figure 3 D,E), indicating that USP7 contributes to overexpression of FGFR1 protein in TPC-1 and SW579 PTC cells. This finding was also further reinforced by using MG132, the repressor of ubiquitin-proteasome,¹⁹ to treat si-USP7-transfected PTC cells. Treatment of MG132 significantly restored FGFR1 protein level reduced by USP7 knockdown in TPC-1 and SW579 PTC cells (Figure 3E). Furthermore, co-transfection of si-USP7 and Flag-FGFR1 plasmid (a FGFR1 expression plasmid fused with Flag tag) resulted in enhanced ubiquitination in Flag-FGFR1 protein in TPC-1 PTC cells (Figure 3F). In addition, immunofluorescence microscopy not only confirmed the positive regulation of USP7 in FGFR1 protein expression but also confirmed the co-localization of USP7 and FGFR1 in TPC-1 PTC cells (Figure 3G). Thus, we conclude that USP7 can stabilize FGFR1 by deubiquitinating FGFR1.

USP7 stabilizes FGFR1 to affect PTC cell growth, invasiveness, migration, and apoptosis

The above data demonstrate that USP7 stabilizes FGFR1 in PTC cells. To elucidate whether the USP7/FGFR1 cascade can regulate PTC cell phenotypes, rescue experiments using co-transfection of a FGFR1 plasmid were carried out in USP7-silenced PTC cells. In TPC-1 and SW579 PTC cells, reduced USP7 expression by si-USP7 introduction caused a significant downregulation

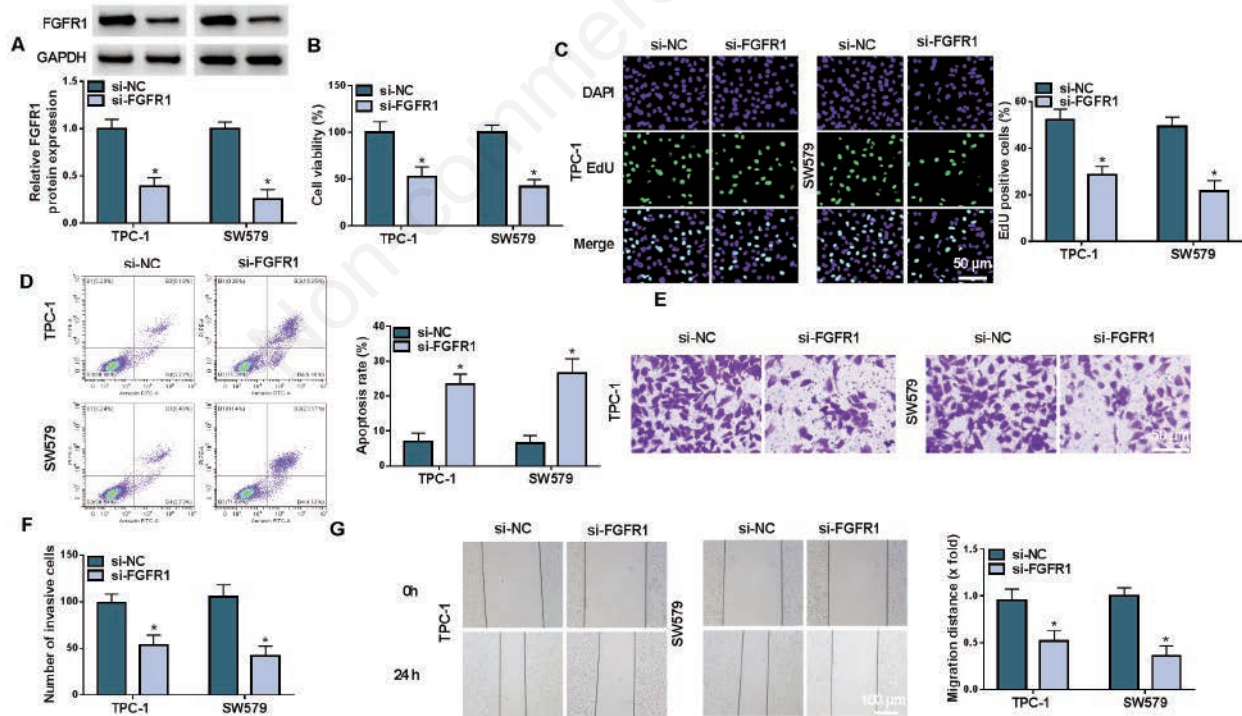


Figure 2. Regulatory functions of FGFR1 in PTC cell phenotypes. **A)** Representative immunoblot showing the protein expression of FGFR1 in TPC-1 and SW579 PTC cells that were introduced with a FGFR1-siRNA (si-FGFR1) or scrambled siRNA sequence (si-NC). **B)** CCK-8 cell viability analysis of TPC-1 and SW579 PTC cells transfected as in A. **C)** EdU cell proliferation assay of TPC-1 and SW579 PTC cells transfected as in A. **D)** Annexin V-FITC and PI staining-based cell apoptosis analysis of TPC-1 and SW579 PTC cells treated as in A. **E,F)** Transwell invasiveness analysis of TPC-1 and SW579 PTC cells introduced as in A. **G)** Wound healing assay of TPC-1 and SW579 PTC cells introduced as in A to test cell migratory ability. * $p < 0.05$.

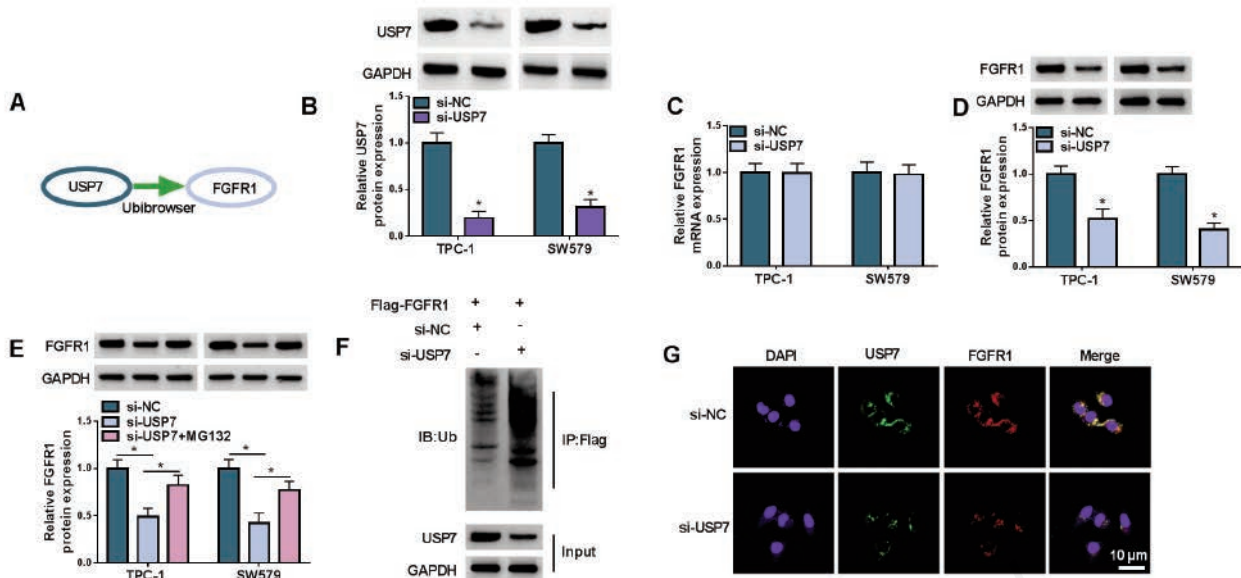


Figure 3. USP7 promotes FGFR1 deubiquitination to stabilize FGFR1 protein. **A)** Ubibrowser 2.0 database predicted the USP7-FGFR1 interaction. **B)** Immunoblots of si-USP7-transfected or si-NC-introduced TPC-1 and SW579 cells for evaluation of USP7 protein expression. **C,D)** FGFR1 mRNA expression analysis by RT-qPCR (**C**) and FGFR1 protein level analysis by immunoblot assay (**D**) in si-USP7-transfected or si-NC-introduced TPC-1 and SW579 cells. **E)** Representative immunoblotting revealing FGFR1 protein level in TPC-1 and SW579 cells after si-NC introduction, si-USP7 transfection, or si-USP7 transfection before MG132 exposure (100 nM, 24 h). **F)** TPC-1 cells were co-transfected with Flag-FGFR1 plasmid and si-USP7 or sh-NC control, followed by immunoprecipitation (IP) experiment with anti-Flag antibody; the immunoprecipitates were subjected to immunoblot assay (IB) using anti-Ub antibody. **G)** Representative immunofluorescence staining depicting the expression and localization of USP7 and FGFR1 in si-USP7-transfected or si-NC-introduced TPC-1 cells. * $p < 0.05$.

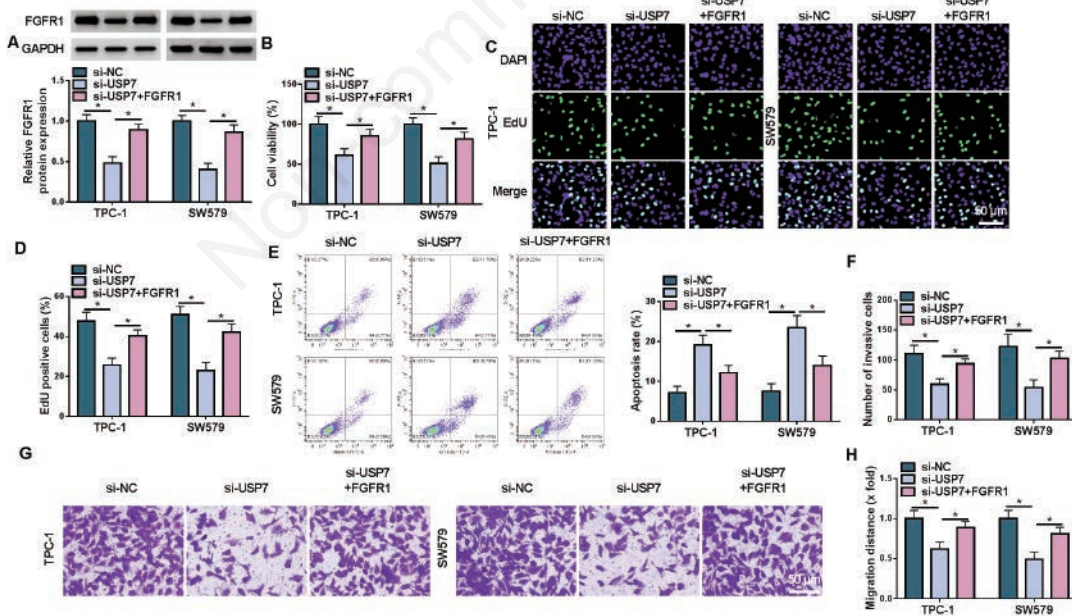


Figure 4. USP7 correlates with PTC cell malignant behaviors by stabilizing FGFR1. **A)** Immunoblots of lysates of TPC-1 and SW579 PTC cells that were introduced with si-USP7, si-USP7+FGFR1 plasmid or scrambled siRNA sequence (si-NC) for evaluation of FGFR1 protein. **B)** Viability analysis of TPC-1 and SW579 PTC cells transfected as in A by CCK-8 assay. **C,D)** Proliferative ability evaluation of TPC-1 and SW579 PTC cells transfected as in A by EdU assay. **E)** Apoptosis analysis of TPC-1 and SW579 PTC cells treated as in A by flow cytometry based Annexin V-FITC and PI staining. **F,G)** Assessment of invasiveness of TPC-1 and SW579 PTC cells introduced as in A by transwell assay. **H)** Determination of migratory ability of TPC-1 and SW579 PTC cells introduced as in A by wound healing assay. * $p < 0.05$.

in FGFR1 protein, which was rescued by this FGFR1 plasmid (Figure 4A). Lessened expression of USP7 led to cell viability and proliferation defects, while FGFR1 re-expression rescued these defects (Figure 4 B-D). Conversely, re-expression of FGFR1 weakened cell apoptosis induced by reduced USP7 expression (Figure 4E). Of note, FGFR1 re-expression also had a counteracting effect on si-USP7-imposed repression of invasiveness and migratory capacity of TPC-1 and SW579 cells (Figure 4 F-H). These data suggest that the USP7/FGFR1 cascade correlates with enhanced PTC malignant behaviors.

YY1 promotes the transcription of FGFR1

The TF YY1 activates the transcription of oncogenic players, thereby contributing to PTC development.¹⁸ Intriguingly, the Jaspas project predicted a potential pairing sequence (CAGAATGGAGGA) for YY1 in the FGFR1 promoter (Figure 5A). Through ChIP experiments with an anti-YY1 antibody, we confirmed the direct binding between YY1 with the FGFR1 promoter (Figure 5B). To investigate the regulatory function of YY1 in FGFR1 transcription, we generated a reporter construct (WT-FGFR1) by inserting the 500-bp length fragment of the FGFR1 promoter harboring the predicted pairing sequence into the pGL3 vector and transfected it into TPC-1 and SW579 cells along with si-YY1, which was validated to silence YY1 expression in both cell lines (Figure 5C). Luciferase assays revealed reduced luciferase activity in cells co-transfected with WT-FGFR1 and si-YY1 compared with si-NC co-transfected cells (Figure 5 D,E). To demonstrate the

validity of the predicted pairing sequence, we also generated a mutation (MUT-FGFR1) carrying a mutated pairing sequence (ACAGCCAAGTTC) (Figure 5A). Downregulation of YY1 did not alter the luciferase activity of cells co-transfected with MUT-FGFR1 (Figure 5 D,E). Indeed, YY1-silenced TPC-1 and SW579 cells exhibited reduced levels of FGFR1 protein (Figure 5F). Thus, YY1 can promote FGFR1 transcription by binding to the FGFR1 promoter *via* the “CAGAATGGAGGA” site.

Downregulation of USP7 prevents xenograft growth *via* FGFR1 reduction

To prove the *in vitro* findings that reduced USP7 expression performs an anti-growth function in PTC cells through FGFR1, we generated SW579 xenograft tumors and conducted the intratumor injection of FGFR1 expression plasmid. The sh-USP7 SW579 xenografts displayed suppressed growth, as evidenced by reduced tumor volume and weight compared with sh-NC controls (Figure 6 A,B). Administration of the FGFR1 plasmid reversed sh-USP7-mediated growth inhibition in SW579 xenografts (Figure 6 A,B). The sh-USP7 SW579 xenografts also exhibited reduced FGFR1 expression, while this FGFR1 plasmid partially abolished the reduction (Figure 6 C,D). In addition, the sh-USP7 SW579 xenografts had fewer Ki67-positive cells than sh-NC controls, while FGFR1 upregulation increased the percentage of the Ki67-positive cells (Figure 6D). These findings confirm that downregulation of USP7 reduces FGFR1 expression, thereby resulting in xenograft growth suppression.

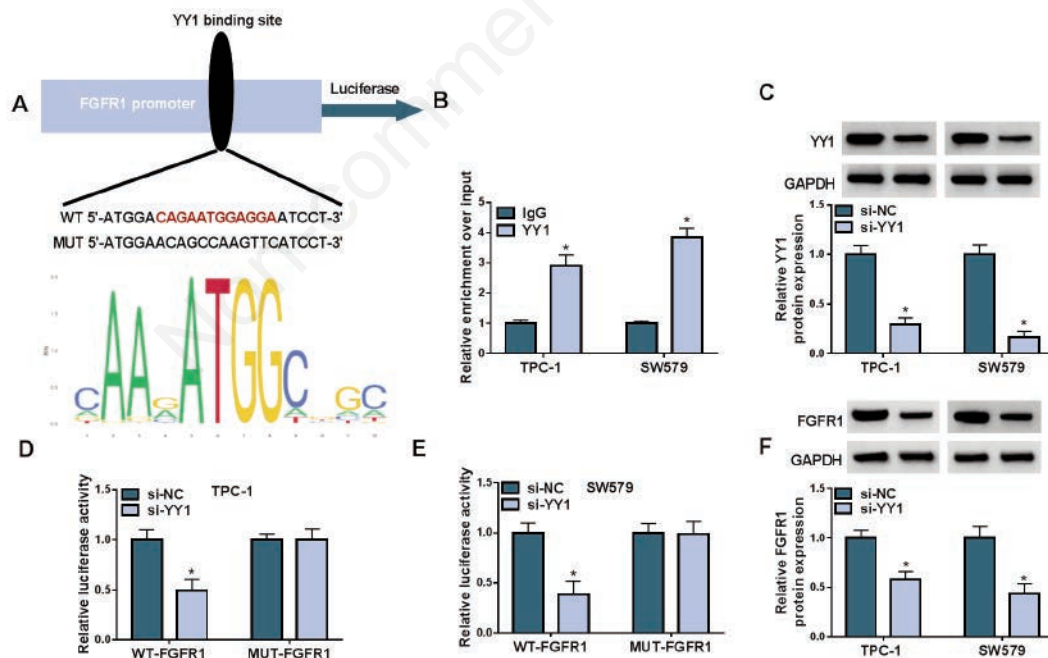


Figure 5. TF YY1 can promote FGFR1 transcription. **A)** Schematic of the motif of YY1, the predicted pairing sequence for YY1 in the FGFR1 promoter, the mutation in the pairing sequence. **B)** ChIP experiments of chromatin of TPC-1 and SW579 cells using antibodies against YY1 and IgG, followed by DNA purification and enrichment analysis of the FGFR1 promoter. **C)** Immunoblots of lysates of si-YY1- or si-NC-transfected TPC-1 and SW579 cells to assess YY1 protein expression. **D,E)** The reporter construct WT-FGFR1 or MUT-FGFR1 was introduced into TPC-1 and SW579 cells along with si-YY1 or si-NC control, followed by analysis of luciferase activity. **F)** Representative immunoblotting showing FGFR1 protein level in si-YY1- or si-NC-introduced TPC-1 and SW579 cells. * $p < 0.05$.

Discussion

FGFR1 possesses significant activity in promoting the tumorigenesis of multiple cancers, including PTC.^{11,13} Inhibition of FGFR1 in cancer cells has been proposed as an anti-cancer option.⁹ Understanding the drivers that contribute to overexpression of FGFR1 could be conducive to exploiting FGFR1 inhibitors. Here, we first confirm the elevated expression and pro-tumorigenic action of FGFR1 in human PTC. Further, we identify the deubiquitinating enzyme USP7 and the oncogenic TF YY1 as inducers of FGFR1 overexpression in PTC.

In agreement with the overexpression in various cancers,⁶⁻⁸ our results have uncovered the elevated expression of FGFR1 mRNA and protein in clinical PTC tumor samples, suggesting the potential role of FGFR1 as a marker for PTC confirmation. FGFR1 has been highlighted as a pro-tumorigenic factor in human carcinogenesis. For example, the FGFR1/MAPK signaling contributes to lung carcinogenesis by promoting immune evasion mediated by PD-L1.⁵ Increased FGFR1 expression underlies the development and

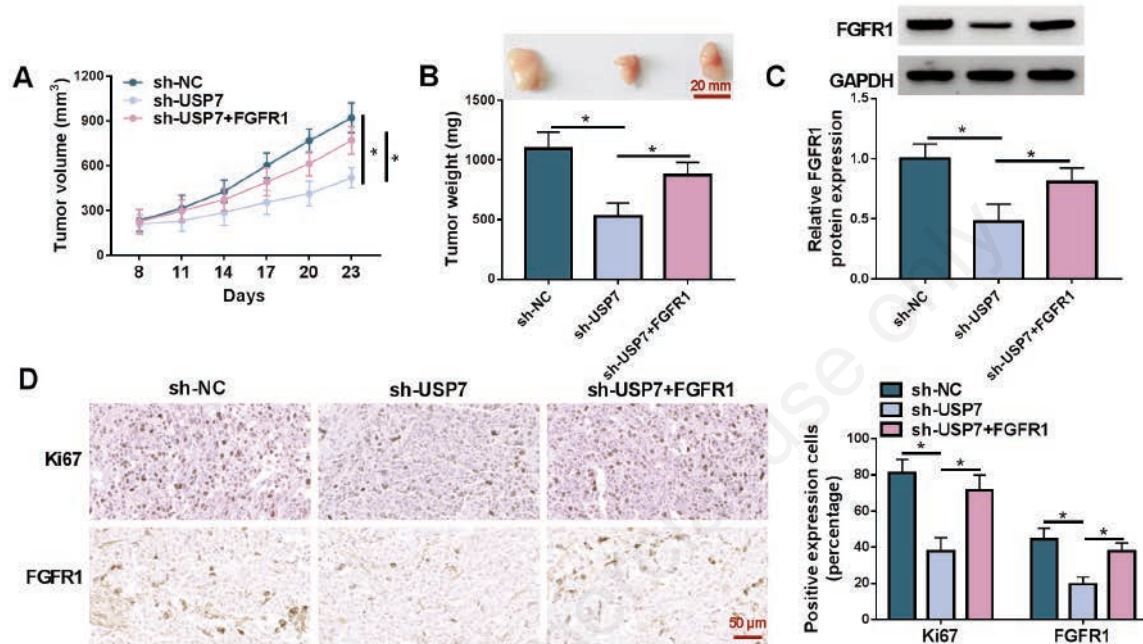


Figure 6 Reduction of USP7 prevents xenograft growth by downregulating FGFR1. **A,B**) Xenograft growth curve (**A**) and weight (**B**) in BALB/c nude mice after injection of sh-NC lentivirus-infected SW579 cells, sh-USP7 lentivirus-transduced SW579 cells with or without intratumor injection of FGFR1 expression plasmid. **C**) Immunoblots of sh-NC SW579 xenografts, sh-USP7 SW579 xenografts and sh-USP7+FGFR1 xenografts to evaluate FGFR1 protein expression. **D**) Representative immunohistochemical staining of xenografts shown in C for evaluation of FGFR1 expression and the Ki67-positive cells. * $p < 0.05$.

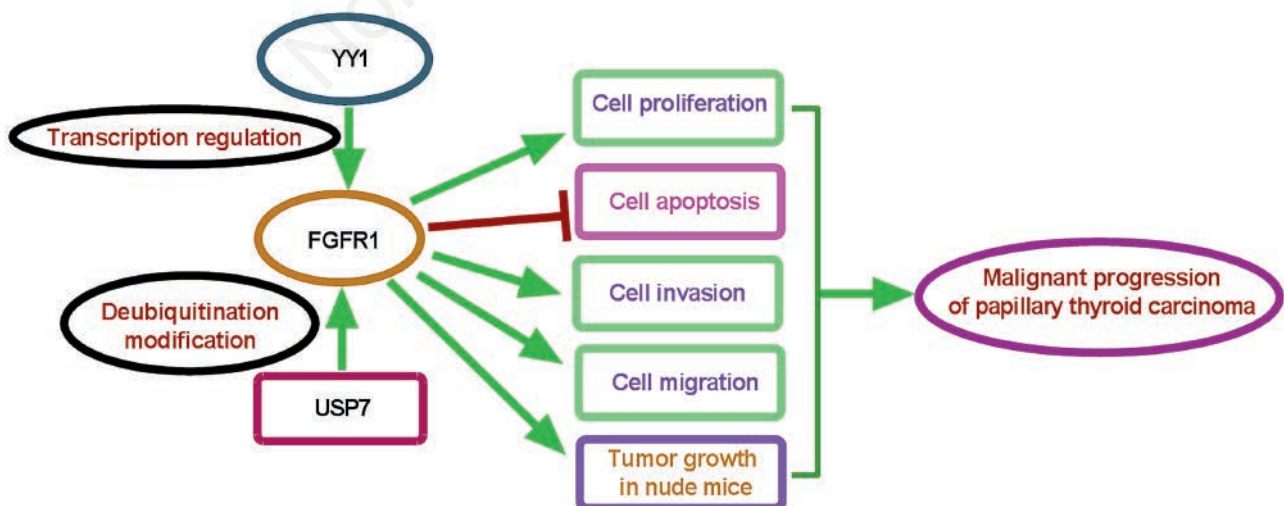


Figure 7. Schematic of the USP7/FGFR1 and YY1/FGFR1 cascades in PTC progression. In PTC cells, the TF YY1 promotes the transcription of FGFR1 and the deubiquitinating enzyme USP7 stabilizes FGFR1, thereby contributing PTC progression

metastasis of prostate cancer.²⁵ Furthermore, overexpression of FGFR1 confers breast cancer cell resistance to the anti-cancer agent metformin, depending on the IRS1/ERK signaling.²⁶ In PTC, FGFR1 can cause enhanced progression by promoting cancer cell metastasis and growth.¹¹ In line with the report, our findings also demonstrate that dysregulated FGFR1 causes PTC development by determining cell malignant phenotypes.

Post-translational modification has garnered great attention for preventing human cancer.²⁷ USP7, a well-known deubiquitinating enzyme, is frequently overexpressed in a number of cancers, and has been identified as a pro-tumorigenic driver by stabilizing oncogenic proteins through deubiquitination.^{23,24} For instance, USP7 deubiquitinates XIAP to enhance protein stability, thereby inhibiting cancer cell apoptosis.²⁸ USP7 is able to enhance cancer cell invasiveness and proliferation by stabilizing EZH2, depending on its deubiquitination.²⁹ USP7 has emerged as a promising target for anti-cancer therapy.³⁰ In PTC, USP7 stabilizes TBX3 by downregulating the ubiquitination and degradation of the TBX3 protein, thus facilitating cancer cell growth.¹⁷ Here, we have pointed out the fact that USP7 can stabilize FGFR1 through deubiquitination. Furthermore, we provide evidence to support that the USP7/FGFR1 cascade contributes to PTC progression.

YY1, a cancer-related TF, functions as a tumor-promoting factor by activating the transcription of oncogenic genes.^{31,32} Previous work has also unveiled the oncogenic effect of YY1 on PTC *via* its pro-transcriptional activity in FOXE1.¹⁸ Through bioinformatics prediction and expression regulation analysis, we have demonstrated, for the first time, that YY1 can promote the transcription and expression of FGFR1 by binding to the FGFR1 promoter. However, the direct evidence of the YY1/FGFR1 cascade in facilitating PTC development is lacking at present. Related research will be warranted in the subsequent exploration.

In summary, as illustrated in Figure 7, we have demonstrated the elevated expression and pro-tumorigenic action of FGFR1 in PTC. Mechanistically, we identify the deubiquitinating enzyme USP7 and the oncogenic TF YY1 as potent inducers of FGFR1 overexpression in PTC. Exploiting inhibitors targeting FGFR1 or its upstream inducers USP7 and YY1 may be foreseen as a potential avenue to control PTC development.

References

- Kitahara CM, Schneider AB. Epidemiology of thyroid cancer. *Cancer Epidemiol Biomarkers Prev* 2022;31:1284-97.
- Wang J, Yu F, Shang Y, Ping Z, Liu L. Thyroid cancer: incidence and mortality trends in China, 2005-2015. *Endocrine* 2020;68:163-73.
- Yuan X, Li Z, Kong Y, Zhong Y, He Y, Zhang A, et al. P65 Targets FGFR1 to regulate the survival of ovarian granulosa cells. *Cells* 2019;8:1334.
- Li D, Xia L, Huang P, Wang Z, Guo Q, Huang C, et al. Cancer-associated fibroblast-secreted IGFBP7 promotes gastric cancer by enhancing tumor associated macrophage infiltration via FGF2/FGFR1/PI3K/AKT axis. *Cell Death Discov* 2023;9:17.
- Hu Y, Lu Y, Xing F, Hsu W. FGFR1/MAPK-directed brachyury activation drives PD-L1-mediated immune evasion to promote lung cancer progression. *Cancer Lett* 2022;547:215867.
- Servetto A, Kollipara R, Formisano L, Lin CC, Lee KM, Sudhan DR, et al. Nuclear FGFR1 regulates gene transcription and promotes antiestrogen resistance in ER(+) breast cancer. *Clin Cancer Res* 2021;27:4379-96.
- Yuan G, Flores NM, Hausmann S, Lofgren SM, Kharchenko V, Angulo-Ibanez M, et al. Elevated NSD3 histone methylation activity drives squamous cell lung cancer. *Nature* 2021;590:504-8.
- Murugesan K, Necchi A, Burn TC, Gjoerup O, Greenstein R, Krook M, et al. Pan-tumor landscape of fibroblast growth factor receptor 1-4 genomic alterations. *ESMO Open* 2022;7:100641.
- Yu T, Yang Y, Liu Y, Zhang Y, Xu H, Li M, et al. A FGFR1 inhibitor patent review: progress since 2010. *Expert Opin Ther Pat* 2017;27:439-54.
- Pfeifer A, Rusinek D, Żebracka-Gala J, Czarniecka A, Chmielik E, Zembala-Nożyńska E, et al. Novel TG-FGFR1 and TRIM33-NTRK1 transcript fusions in papillary thyroid carcinoma. *Genes Chromosomes Cancer* 2019;58:558-66.
- Liu W, Zhao J, Jin M, Zhou M. circRAPGEF5 contributes to papillary thyroid proliferation and metastasis by regulation miR-198/FGFR1. *Mol Ther Nucleic Acids* 2019;14:609-16.
- Han S, Wang R, Zhang Y, Li X, Gan Y, Gao F, et al. The role of ubiquitination and deubiquitination in tumor invasion and metastasis. *Int J Biol Sci* 2022;18:2292-303.
- Zheng L, Tang T, Wang Z, Sun C, Chen X, Li W, et al. FUS-mediated CircFGFR1 accelerates the development of papillary thyroid carcinoma by stabilizing FGFR1 protein. *Biochem Genet* 2024. Online Ahead of Print.
- Lambert SA, Jolma A, Campitelli LF, Das PK, Yin Y, Albu M, et al. The human transcription factors. *Cell* 2018;172:650-65.
- Qin X, Jiang Q, Komori H, Sakane C, Fukuyama R, Matsuo Y, et al. Runt-related transcription factor-2 (Runx2) is required for bone matrix protein gene expression in committed osteoblasts in mice. *J Bone Miner Res* 2021;36:2081-95.
- Henning NJ, Boike L, Spradlin JN, Ward CC, Liu G, Zhang E, et al. Deubiquitinase-targeting chimeras for targeted protein stabilization. *Nat Chem Biol* 2022;18:412-21.
- Xie P, Wang H, Xie J, Huang Z, Chen S, Cheng X, et al. USP7 promotes proliferation of papillary thyroid carcinoma cells through TBX3-mediated p57(KIP2) repression. *Mol Cell Endocrinol* 2020;518:111037.
- Li S, Zhang Z, Peng H, Xiao X. YY1-induced up-regulation of FOXE1 is negatively regulated by miR-129-5p and contributes to the progression of papillary thyroid microcarcinoma. *Pathol Res Pract* 2021;221:153337.
- Sulkshane P, Duek I, Ram J, Thakur A, Reis N, Ziv T, et al. Inhibition of proteasome reveals basal mitochondrial ubiquitination. *J Proteomics* 2020;229:103949.
- Hu Z, Chen G, Zhao Y, Gao H, Li L, Yin Y, et al. Exosome-derived circCCAR1 promotes CD8+T-cell dysfunction and anti-PD1 resistance in hepatocellular carcinoma. *Mol Cancer* 2023;22:55.
- Yao B, Zhang Q, Yang Z, An F, Nie H, Wang H, et al. CircEZH2/miR-133b/IGF2BP2 aggravates colorectal cancer progression via enhancing the stability of m(6)A-modified CREB1 mRNA. *Mol Cancer* 2022;21:140.
- Wang X, Li Y, He M, Kong X, Jiang P, Liu X, et al. UbiBrowser 2.0: a comprehensive resource for proteome-wide known and predicted ubiquitin ligase/deubiquitinase-substrate interactions in eukaryotic species. *Nucleic Acids Res* 2022;50:D719-28.
- Saha G, Roy S, Basu M, Ghosh MK. USP7 - a crucial regulator of cancer hallmarks. *Biochim Biophys Acta Rev Cancer* 2023;1878:188903.
- Korenev G, Yakukhnov S, Druk A, Golovina A, Chasov V, Mirgayazova R, et al. USP7 inhibitors in cancer immunotherapy: current status and perspective. *Cancers (Basel)* 2022;14:5539.
- Yang F, Zhang Y, Ressler SJ, Ittmann MM, Ayala GE, Dang TD, et al. FGFR1 is essential for prostate cancer progression

- and metastasis. *Cancer Res* 2013;73:3716-24.
26. Shi Y, Ma Z, Cheng Q, Wu Y, Parris AB, Kong L, et al. FGFR1 overexpression renders breast cancer cells resistant to metformin through activation of IRS1/ERK signaling. *Biochim Biophys Acta Mol Cell Res* 2021;1868:118877.
 27. Han ZJ, Feng YH, Gu BH, Li YM, Chen H. The post-translational modification, SUMOylation, and cancer (Review). *Int J Oncol* 2018;52:1081-94.
 28. Saha G, Sarkar S, Mohanta PS, Kumar K, Chakrabarti S, Basu M, et al. USP7 targets XIAP for cancer progression: Establishment of a p53-independent therapeutic avenue for glioma. *Oncogene* 2022;41:5061-75.
 29. Zheng N, Chu M, Lin M, He Y, Wang Z. USP7 stabilizes EZH2 and enhances cancer malignant progression. *Am J Cancer Res* 2020;10:299-313.
 30. Carreira LD, Oliveira RI, Moreira VM, Salvador JAR. Ubiquitin-specific protease 7 (USP7): an emerging drug target for cancer treatment. *Expert Opin Ther Targets* 2023;27:1043-58.
 31. Li B, Wang J, Liao J, Wu M, Yuan X, Fang H, et al. YY1 promotes pancreatic cancer cell proliferation by enhancing mitochondrial respiration. *Cancer Cell Int* 2022;22:287.
 32. Tseng HY, Chen YA, Jen J, Shen PC, Chen LM, Lin TD, et al. Oncogenic MCT-1 activation promotes YY1-EGFR-MnSOD signaling and tumor progression. *Oncogenesis* 2017;6:e313.

Non-commercial use only

Received: 16 April 2024. Accepted: 3 July 2024.

This work is licensed under a Creative Commons Attribution-NonCommercial 4.0 International License (CC BY-NC 4.0).

©Copyright: the Author(s), 2024

Licensee PAGEPress, Italy

European Journal of Histochemistry 2024; 68:4048

doi:10.4081/ejh.2024.4048

Publisher's note: all claims expressed in this article are solely those of the authors and do not necessarily represent those of their affiliated organizations, or those of the publisher, the editors and the reviewers. Any product that may be evaluated in this article or claim that may be made by its manufacturer is not guaranteed or endorsed by the publisher.